

Low Level Control of a Quadrotor with Deep Model-Based Reinforcement Learning

Nathan O. Lambert¹, Daniel S. Drew¹, Joseph Yaconelli², Roberto Calandra¹, Sergey Levine¹, and Kristofer S. J. Pister¹

Abstract—Generating low-level robot controllers often requires manual parameters tuning and significant system knowledge, which can result in long design times for highly specialized controllers. With the growth of automation, the need for such controllers might grow faster than the number of expert designers. To address the problem of rapidly generating low-level controllers without domain knowledge, we propose using model-based reinforcement learning (MBRL) trained on few minutes of automatically generated data. In this paper, we explore the capabilities of MBRL on a Crazyflie quadrotor with rapid dynamics where existing classical control schemes offer a baseline against the new method’s performance. To our knowledge, this is the first use of MBRL for low-level controlled hover of a quadrotor using only on-board sensors, direct motor input signals, and no initial dynamics knowledge. Our forward dynamics model for prediction is a neural network tuned to predict the state variables at the next time step, with a regularization term on the variance of predictions. The model predictive controller then transmits best actions from a GPU-enabled base station to the quadrotor firmware via radio. In our experiments, the quadrotor achieved hovering capability of up to 6 seconds with 3 minutes of experimental training data.

I. INTRODUCTION

The design of appropriate robot controllers is traditionally a time-consuming and expert-based process. Even for relatively simple systems such as a quadrotor, tuning the parameters of the low-level PID controller can be challenging and often results in sub-optimal controllers. Control frequency and tuning becomes even more critical as the vehicle size decreases due to the subsequent change in the highly non-linear dynamics of the system. In this paper, we investigate the question: Is it possible to autonomously learn competitive low-level controllers for a quadrotor from scratch, i.e., without bootstrapping or demonstration? To answer this question, we turn to model-based reinforcement learning (MBRL) – a compelling approach to synthesize controllers even for systems without analytic dynamics models and with high cost per experiment [1]. Our contribution builds on simulated results in MBRL [2] and the application of the MBRL framework to quadrupeds [3], as it is the first demonstration of controlling a passively unstable system with rapid dynamic using the model-based system only learning via experience. While related applications of learning with quadrotors employ a low-level controller for a quadrotor generated in simulation [4] or use a dynamics model learned via

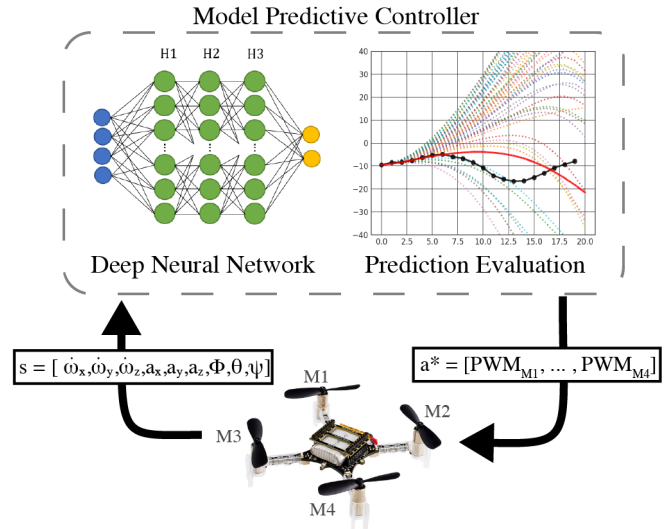


Fig. 1: The closed loop model predictive controller used to stabilize the Crazyflie. Using deep model-based reinforcement learning, the quadrotor reach stable hovering with only 10,000 trained datapoints – equivalent to 3 minutes of flight.

experience to provide set-points for on-board controllers [5], our work is the first to control flight via a low-level controller trained only on experimental data.

MBRL has been shown to operate in a data-efficient manner to control robotic systems by iteratively learning a dynamics model and subsequently leveraging it to design controllers [6], [7]. Our MBRL solution, outlined in Figure 1, employs deep neural networks to learn a forwards dynamics model, coupled with a ‘random shooter’ model predictive controller (MPC) similar to the one evaluated in simulation by [2]. This approach can be efficiently parallelized on a graphic processing unit (GPU) to execute low-level, real-time control. Using this approach, we demonstrate on the Crazyflie (an established commercial quadrotor often used for research) the controlled hover of a quadrotor directly from raw sensor measurements and application of pulse width modulation (PWM) motor signals.

The resulting system achieves repeated stable hover of up to 6 seconds, with failures due to drift of unmeasured states, within 3 minutes of fully-autonomous training data, demonstrating the ability of MBRL to control robotic systems in the absence of: any a priori knowledge of dynamics; any pre-configured internal controllers for stability or actuator response smoothing; and any expert demonstration.

Corresponding author: Nathan O. Lambert nol@berkeley.edu

¹Department of Electrical Engineering and Computer Sciences, University of California, Berkeley.

²Author is supported by the Berkeley SUPERB REU Program. Author is affiliated with Department of Computer Science, University of Oregon.

II. RELATED WORK

A. Attitude and Hover Control of Quadrotors

Classical controllers (e.g., PID) in conjunction with analytic models for the rigid body dynamics of a quadrotor are often sufficient to control vehicle attitude [8]. In addition, linearized models are sufficient to simultaneously control for global trajectory, stable hover, and attitude setpoint using well-tuned nested PID controllers [9]. Standard control approaches show impressive acrobatic performance with quadrotors, but are heavily domain specific and can take many hours to fine tune. The goal of MBRL is to highlight a competitive solution that generates a functional controller in less time with no foundation of dynamics knowledge.

Research focusing on developing novel low-level attitude and hover controllers shows functionality in extreme nonlinear cases, such as for quadrotors with a missing propeller [10], with multiple damaged propellers [11], or with the capability to dynamically tilt its propellers [12]. Optimal control schemes have demonstrated results on standard quadrotors with extreme precision and robustness [13].

Our work differs by specifically demonstrating the possibility of attitude and hover control via real-time external MPC. Unlike other work on real-time MPC for quadrotors [14], [15], ours uses a dynamics model derived fully from in-flight data (i.e., with no a priori structure or terms) that takes motors signals as direct inputs. Effectively, our model encompasses only the actual dynamics of the system, while other implementations also incorporate the dynamics of previously existing internal controllers as well. The general nature of our model from sensors to actuators curates the potential for use on robots with no previous controller - we only use the quadrotor as the basis for comparison and do not expect it to be the limits of the MBRL system's functionality.

B. Learning for Quadrotors

Although learning-based approaches have been widely applied for trajectory control of quadrotors, implementations typically rely on sending controller outputs as setpoints to stable on-board attitude and thrust controllers. Iterative learning control (ILC) approaches [16], [17] have demonstrated robust control of quadrotor flight trajectories but require higher frequency on-board controllers for attitude setpoints. Learning-based model predictive control implementations which successfully track trajectories also wrap their control around on-board attitude controllers by directly sending Euler angle or thrust commands [18], [19]. Gaussian process-based automatic tuning of position controller gains has been demonstrated [20], but only in parallel with on-board motor thrust and attitude controllers tuned separately.

Model-free reinforcement learning has been shown to generate control policies for quadrotors that out-perform linear MPC controllers [4]. Although similarly motivated by a desire to generate a control policy acting directly on actuator inputs, this work used an external vision system for state error correction, operated with an internal motor speed controller enabled (i.e., thrusts were commanded and

not motor voltages), and generated a large fraction of its data in simulated rollouts.

Researchers of system identification for quadrotors also apply machine learning techniques. Bansal et al. used neural network models of the Crazyflie's dynamics to plan trajectories [5]. Our implementation differs by directly predicting change in attitude (e.g. body pose, angular rates) based on raw actuator signals.

Using Bayesian Optimization to learn a linearized quadrotor dynamics model demonstrated capabilities for tuning of an optimal control scheme [21]. While this approach is data-efficient and is shown to outperform analytic models, the model learned is task-dependent.

C. Model-based Reinforcement Learning

Functionality of MBRL is evident in simulation for multiple tasks in low data regimes, including quadrupeds [22] and manipulation tasks [23]. Low-level MBRL control (i.e., with direct motor input signals) of an RC car has been demonstrated experimentally, but the system is of much lower dimensionality and has passive stability [24]. Relatively low-level control (i.e., mostly thrust commands only passed through an internal governor before conversion to motor signals) of an autonomous helicopter has been demonstrated, but required a ground-based vision system for error correction in state estimates as well as expert demonstration for model training.

Properly optimized neural networks trained on experimental data shows test error below common analytic dynamics models for flying vehicles, but the models did not include direct actuator signals and did not include experimental validation through controller implementation [25]. A model predictive path integral (MPPI) controller using a learned neural network demonstrated data-efficient trajectory control of a quadrotor, but results were only shown in simulation and required the network to be initialized with 30 minutes of demonstration data with pre-engineered controllers [7].

MBRL with trajectory sampling for control outperforms, in terms of samples needed for convergence, the asymptotic performance of recent model free algorithms in low dimensional tasks [2]. Our work builds on strategies presented, with most influence derived from work on "probabilistic" neural networks, to demonstrate functionality in an experimental setting - i.e., in the presence of real-world higher order effects, variability, and time constraints).

Neural network-based learned dynamics models with model predictive control have functions for experimental control of an under-actuated hexapod [3]. The hexapod platform does not have the same requirements on frequency or control error due to its passive stability, and incorporates a GPS unit for relatively low-noise state measurements. Our work has a similar architecture, but has improvements in the network model and model predictive controller to allow substantially higher control frequencies with noisy state data. By demonstrating functionality without global positioning data, the procedure can be extended to more robot platforms where

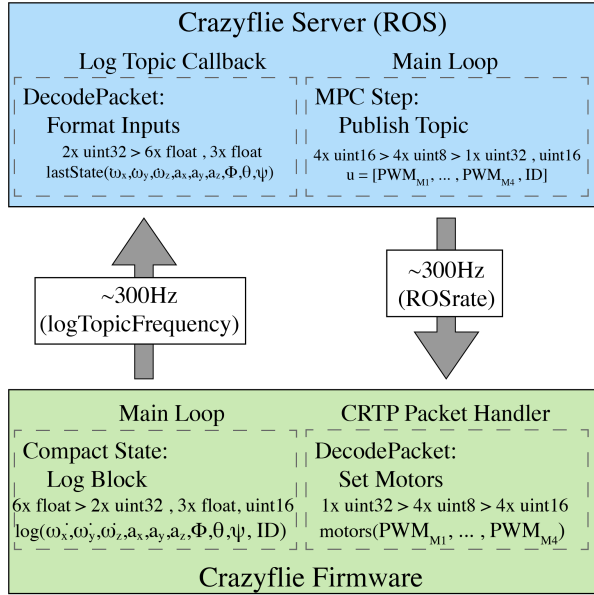


Fig. 2: The ROS system and the Crazyflie communicate in an minimal fashion. The ROS side computer passes control signals and state data between the model predictive controller node and the Crazyflie ROS server. The Crazyflie server packages Tx PWM values to send and unpacks Rx compressed log data from the robot.

only internal state and actuator commands are available to create a dynamics model and control policy.

III. EXPERIMENTAL SETUP

In this paper, we use as experimental hardware platform the open-source Crazyflie 2.0 quadrotor [26]. The Crazyflie is 27 g and 9 cm², so the rapid system dynamics create a need for a high speed controller; by default, the internal PID controller used for attitude control runs at 500 Hz, with Euler angle state estimation updates at 1 kHz. This section specifies the system involved in controlling the quadrotor and the firmware modifications required for external stability control.

All components we used are based on publicly available and open source projects. We used the Crazyflie ROS interface supported here: github.com/whoenig/crazyflie_ros. This interface allows for easy modification of the radio communication and employment of the learning framework. Our ROS structure is simple, with a Crazyflie subscribing to PWM values generated by a controller node, which processes radio packets sent from the quadrotor in order to pass state variables to the model predictive controller (as shown in Figure 2). The Crazyradio PA USB radio is used to send commands from the ROS server; software settings in the included client increase the maximum data transmission bitrate up to 2 Mbps and a Crazyflie firmware modification improves the maximum traffic rate from 100 Hz to 400 Hz.

In packaged radio transmissions from the ROS server we define actions directly as the pulse-width modulation (PWM) signals sent to the motors. To assign these PWM

values directly to the motors we bypass the controller updates in the standard Crazyflie firmware by changing the motor power distribution whenever a CRTP Commander packet is received (see Figure 2) instead of modifying a controller setpoint value. The Crazyflie ROS package sends empty ping packets to the Crazyflie to ask for logging data in the returning acknowledgment packet; without decreasing the logging payload and rate we could not simultaneously transmit PWM commands at the desired frequency due to radio communication constraints. We created a new internal logging block of compressed IMU data and Euler angle measurements to decrease the required bitrate for logging state information, trading state measurement precision for update frequency. Action commands and logged state data are communicated asynchronously; the ROS server control loop has a frequency set by the ROS rate command, while state data is logged based on a separate ROS topic frequency. To verify control frequency and reconstruct state action pairs during autonomous rollouts we use a round-trip packet ID system. The controller will not send another command until the Crazyflie logging confirms that the PWM ID from the (at most two) prior MPC update has been set to the motors. This check confirms that a radio delay or buffer growth will not propagate through the system.

IV. LEARNING FORWARD DYNAMICS

Generating a dynamics model for the robot requires training a neural network to fit a parametric function f_θ to predict the next state of the robot as a discrete change in state $s_{t+1} = s_t + f_\theta(s_t, a_t)$. In training, using a probabilistic loss function with a penalty term on the variance of estimates better clusters predictions for more stable predictions across multiple time-steps [2].

The probabilistic loss function assisted model convergence and the variance penalty helps maintain stable predictions on longer time horizons. Our networks train with the Adam optimizer [27] for 60 epochs with a learning rate of .0005 and a batch size of 32. The network design is summarized in Figure 3. All layers except for the output layer use the Swish activation function [28] with parameter $\beta = 1$.

Training a probabilistic neural network to approximate the dynamics model requires pruning of logged data (e.g.

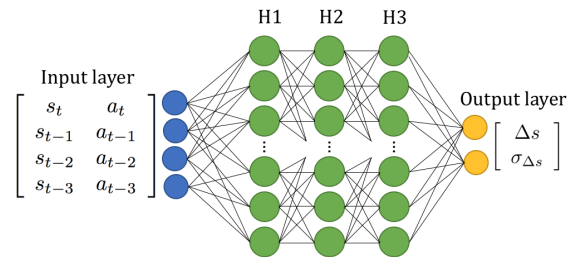


Fig. 3: The neural network dynamics model consists of the past 4 state-action pairs predicting the mean and variance of the change in state. The input is of dimension 52, predicting an 18 dimensional output. We use 2 hidden layers of width 250, with the Swish activation function.

dropped packets) and scaling of variables to assist model convergence. Our state model s_t is the vector of Euler angles (i.e., yaw, pitch, and roll or ϕ, θ, ψ), linear accelerations ($\ddot{x}, \ddot{y}, \ddot{z}$), and angular accelerations ($\dot{\omega}_x, \dot{\omega}_y, \dot{\omega}_z$)

$$s_t = [\dot{\omega}_x, \dot{\omega}_y, \dot{\omega}_z, \phi, \theta, \psi, \ddot{x}, \ddot{y}, \ddot{z}]^T. \quad (1)$$

The Euler angles are from the Crazyflie internal complementary filter while the linear and angular accelerations are measured directly from the on-board MPU-9250 9-axis IMU. In practice, for predicting across longer time horizons, modeling acceleration values as a global next state, rather than a change in state from the current measurement, increased the length of time horizon in composed predictions before the models diverged. While the change in Euler angle predictions are stable, the change in raw accelerations vary widely with sensor noise and cause non-physical dynamics predictions, so all the linear and angular accelerations are trained to fit the global next state.

We combine the state data with the four PWM values, $a_t = [m_1, m_2, m_3, m_4]^T$, to get the system information at time t . The neural networks are cross-validated to confirm using all state data (i.e., including the relatively noisy raw gyroscope and accelerometer measurements) improves prediction accuracy in the change in state. The one step predictions for our final model is shown in Figure 4.

While the dynamics for a quadrotor are often represented as a linear system of equations, for a MAV at high control frequencies motor step response and thrust asymmetry heavily impact the change in state, resulting in a heavily nonlinear dynamics model. The step response of a Crazyflie motor from PWM 0 to max is on the order of 250 ms, so our update time-step of 20 ms is short enough for motor spin-up to contribute significantly to learned dynamics. To account for spin-up, we append past system information to the current state and PWMs to generate an input into the neural network model that includes past time. From the exponential step response and with a bounded possible PWM value within $p_{eq} \pm 5000$, the motors need approximately 25 ms to reach the desired rotor speed; when operating at 50 Hz, the time step between updates is 20 ms, leading us to an appended states and PWMs history of length 4. This state action history length was validated as having the lowest test error on our data-set (lengths 1 to 10 evaluated). This yields the final input to our neural network, ξ , being of length 52, with 4 state and action vectors concatenated as

$$\xi_t = [s_t \ s_{t-1} \ s_{t-2} \ s_{t-3} \ a_t \ a_{t-1} \ a_{t-2} \ a_{t-3}]^T. \quad (2)$$

V. CONTROL ALGORITHM

Model predictive control provides a framework for evaluating many action candidates using a given dynamics model. We employ a ‘random shooter’ MPC, where a set of N randomly generated actions are simulated over a time horizon T . The best action is decided by a user designed objective function that takes in the simulated trajectories $\hat{X}(a, s_t)$ and returns a best action, a^* ; as visualized in Figure 5. The candidate actions are 4-tuples of motor PWM values centered

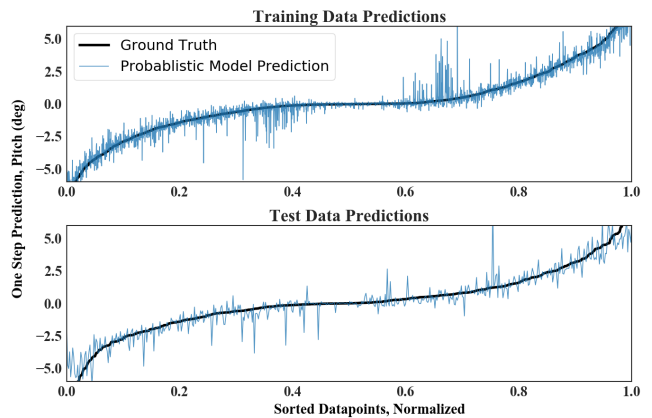


Fig. 4: The one step predictions of our model for Pitch. The x-axis is indices of the sorted ground truth value for change in pitch from the previous time-step. The training data, top, and the testing data, bottom, track the one step forward dynamics, but suffer from high noise. The similarity of the noise on the training and test data indicate a difficult system to model due to system noise, rather than over or under-fitting the validation data.

around the stable hover-point for the tested Crazyflie. The 4 PWM values in one sample action $a_i = (a_{i,1}, a_{i,2}, a_{i,3}, a_{i,4})$, where the index $i = 1, 2, \dots, N$. The candidate actions are constant across the time horizon T . For a single sample a_i , each $a_{i,j}$ is chosen from a uniform random variable on the interval $[p_{eq,j} - \sigma, p_{eq,j} + \sigma]$, where $p_{eq,j}$ is the equilibrium PWM value for motor j . The range of the uniform distribution is controlled by the tuned parameter σ ; this has the effect of restricting the variety of actions the Crazyflie can take. For the given range of PWM values for each motor, $[p_{eq} - \sigma, p_{eq} + \sigma]$, we discretize the candidate PWM values to a step size of 256 to match the future compression into a radio packet. This discretization of available action choices also increases the coverage of the 4-dimensional candidate action space without an increase in N that would lead to decreased control frequency.

The objective function we designed for stability seeks to minimize distance from the origin for pitch and roll, while adding additional cost terms to Euler angle rates. The omission of global yaw term is because yaw does not reset to 0 at each takeoff and seeking a yaw of zero is not necessary for stability.

$$a^* = \arg \min_a c(\hat{X}(a, s_t)) \quad (3)$$

$$= \arg \min_a \sum_{t=1}^T \lambda_\theta (\psi_t^2 + \theta_t^2) + \lambda_\nabla (\dot{\psi}_t^2 + \dot{\theta}_t^2 + \dot{\phi}_t^2). \quad (4)$$

In this objective function, λ_θ maps roughly to a proportional, or gain, term and λ_∇ corresponds to a derivative, or damping, term. Adding cost terms to predicted accelerations did not improve performance because of the inconsistency of the predictions towards the end of the time horizon $T > 5$.

Our MPC operates on a time horizon $T = 12$ to leverage the predictive power of our model. Higher control frequen-

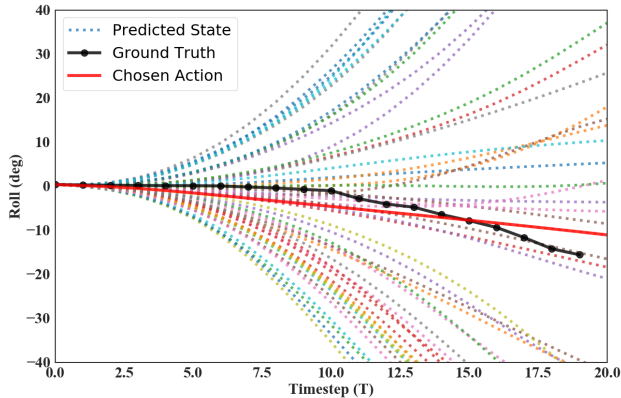


Fig. 5: Each line is a predicted future state from a candidate action, $N = 50$ here, with the chosen “best action” highlighted in red. For our experiments we used a time horizon of $T = 12$, but further in the future is plotted. The future evolution of the roll of the quadrotor is plotted in black to show that the predictions of the chosen action matches the state change for $T < 3$. The prediction is expected to diverge at future times because actions are re-planned at every step.

cies can run at a cost of prediction horizon, such as $T = 9$ at 75 Hz or $T = 6$ at 100 Hz. In the extreme case, at $T = 1$, the controller can run over 200 Hz, but at high frequencies we do not have reliable derivative information on our predictions and dynamics models are less accurate due to the smaller state change, so it is difficult to make suitable actions. For our experiments at 50 Hz, the predictive power is strong, but the relatively low control frequencies lends the controller to be susceptible to disturbances in between control updates. Figure 5 shows how the model predictions diverge over time. At 50 Hz, a time horizon of 12 corresponds to a prediction of 240 ms into the future. Assessing flight beyond 240 ms is not guaranteed to improve performance, but further exploration of the trade off between number of samples, time horizon, and frequency is warranted. A system running with an Nvidia Titan Xp holds a maximum control frequency of 230 Hz with $N = 5000, T = 1$. For testing we use a locked frequencies of 25 Hz and 50 Hz at $N = 5000, T = 12$. Our control algorithm is summarized in Algorithm 1.

VI. EXPERIMENTAL EVALUATION

We now describe the setting used in our experiments, the learning process of the system, and the performance summary of the control algorithm. Videos of the flying quadrotor, and full code for controlling the Crazyflie and reproducing the experiments are available online at <https://sites.google.com/berkeley.edu/mbri-quadrotor/>.

A. Experimental Setting

The performance of our controller is measured by the average flight length over each roll-out. An example flight with clear controlled Euler angles is shown in Figure 9. Failure is primarily due to collision with an object due to drift, or, as in many earlier roll-outs, when flights reach a pitch or roll angle over 40° . In both cases, an emergency stop

Algorithm 1 ROS MPC Summary

```

1: Gather random data  $\mathbb{D}_0$ , train initial model  $f_{0,\theta}$ 
2: for roll-out  $r = 1$  to  $R$  do
3:   while Flying do
4:     ROS Rx:  $(s_t, a_t)$ 
5:     Compile  $\xi_t = [s_t, a_t, \dots, s_{t-3}, a_{t-3}]$ 
6:     for  $i = 1$  to  $N$  do
7:        $\{a\}_{i,j} \sim U(p_{eq,j} - \sigma, p_{eq,j} + \sigma)$ 
8:       for  $k = 1$  to  $T$  do
9:          $s_{t+k} = s_{t+k-1} + f_{i,\theta}(\xi_t)$ 
10:      end for
11:       $obj(a_i) = \sum_{k=1}^T c(s_{t+k}, a_i)$ 
12:    end for
13:    ROS Tx:  $a^* = \arg \min_a obj(a_i)$ 
14:  end while
15:  Append data  $\mathbb{D} = \mathbb{D}_r \cup \dots \cup \mathbb{D}_0$ , train  $f_{r,\theta}$  on  $\mathbb{D}$ 
16: end for

```

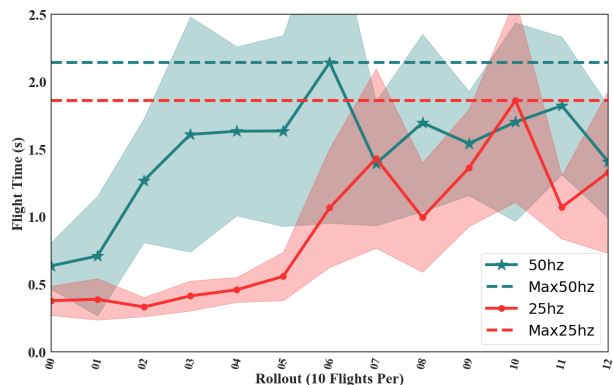


Fig. 6: Mean and standard deviation of the 10 flights during each flight for learning at 25 Hz and 50 Hz. The 50 Hz shows a slight edge on final performance, but a much quicker learning ability per flight by having more PWM switches during control.

command is automatically sent to the motors to minimize quadrotor damage during data collection. Along with the collisions due to drift, the simple onboard state estimator shows heavy drift on the Euler angles following a rapid throttle ramping; both are limiting factors on the length of controlled flight without a dead reckoning system. Notably, the quadrotor with internal PIDs on will still fail regularly due to drift on the same time frame as our controller; it is only when external inputs are given that the internal controllers will obtain substantially longer flights. The drift showcases the challenge of attitude based controllers to mitigate an offset in velocity.

B. Learning Process

The learning process follows the reinforcement learning framework of collecting data and iteratively updating the policy. We trained an initial model f_0 on 124 and 394 points of dynamics data at 25 Hz and 50 Hz, respectively, from the Crazyflie being flown by a random action controller supplying PWM values. Starting with this initial model as the

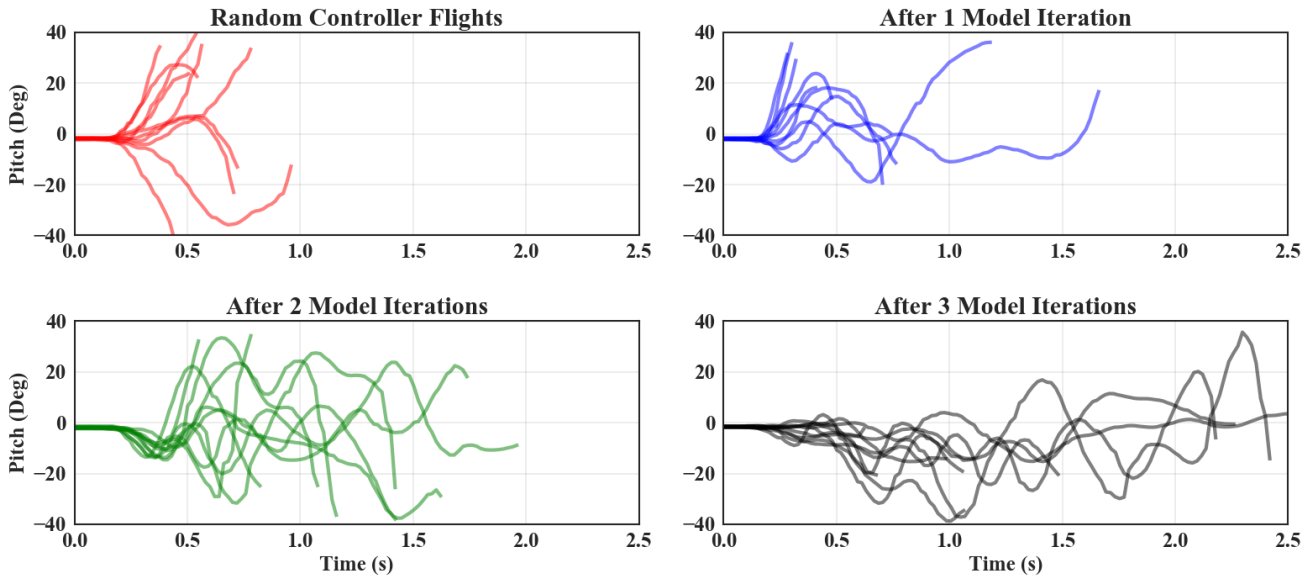


Fig. 7: The pitch over time for each flight in the first four roll-outs of learning at 50 Hz, showing the rapid increase in control ability on limited data. The random and first controlled roll-out show little ability to correct, but roll-out 3 is already progressing multiple flights beyond 2 seconds.

MPC plant, the Crazyflie undertakes a series of autonomous flights from the ground with a 250 ms ramp up, open-loop takeoff followed by on-policy control while logging data to the ROS base-station. Each roll-out is a series of 10 flights, which causes large variances in flight time. The initial roll-outs have less control authority and inherently explore more unstable state spaces, which is valuable to future iterations that wish to recover from higher pitch and or roll. The random and first three controlled roll-outs are plotted in Figure 7 to show the rapid improvement of performance with very little training data. The full learning curves are showing in Figure 6, where the rapid visible improvement in results is evident. Both at 25 Hz and 50 Hz the rate of flight improvement reaches its maximum rate once there is 1,000 trainable points for the dynamics model, which takes longer to collect at the lower control frequency.

Both 25 Hz and 50 Hz control show a level off in performance after reaching a certain data threshold. The longest individual flights during these roll-outs is over 5 s for both frequencies. The leveling off could be caused by a slow in improvement of the dynamics model, with orders of magnitude growth in amount of data potentially being needed for further performance improvements. The final models at 25 Hz and 50 Hz are trained on 2,608 and 9,655 points respectively, but best performances are achieved before the final models.

C. Performance Summary

This controller demonstrates the ability to hover, following a “clean” open-loop takeoff, for multiple seconds. At both 25 Hz and 50 Hz, once reaching maximum performance in the 12 roll-outs, about 30% of flights fail to drift. The failures due to drift indicate the full potential of the MBRL solution to low-level quadrotor control. An example of a segment test

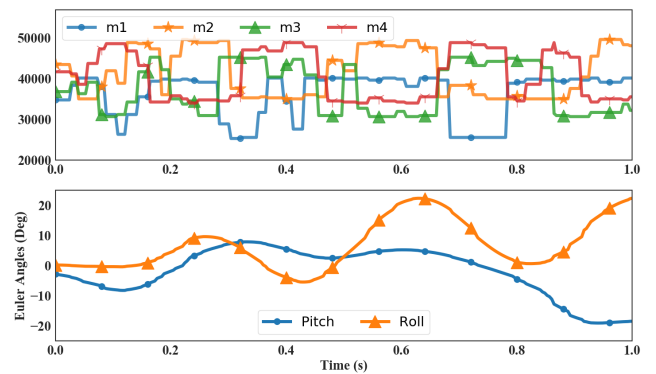


Fig. 8: The performance of the 50 Hz controller during a flight segment. The total time under control for this flight is over 5 s. Above: The controlled PWM values over time, which visibly change in response to angle oscillations. Below: Controlled pitch and roll.

flight is shown in Figure 8, where the response to pitch and roll error is visible in the PWM signal.

The system has multiple limitations resulting in the short time-scale and high variance of flights. First, the PWM equilibrium values of the motors shift by over 10% following a strong collision, causing the true dynamics model to shift semi-randomly over time. Additionally, the internal state estimator does not track extreme changes in Euler angles accurately; our controller, which operates at a relatively low rate for motor control, needs carefully tuned damping terms to eliminate oscillations from open loop takeoff or control overshoot. We believe that overcoming the system-level and dynamical limitations of controlling the Crazyflie in this manner showcase the expressive power of MBRL.

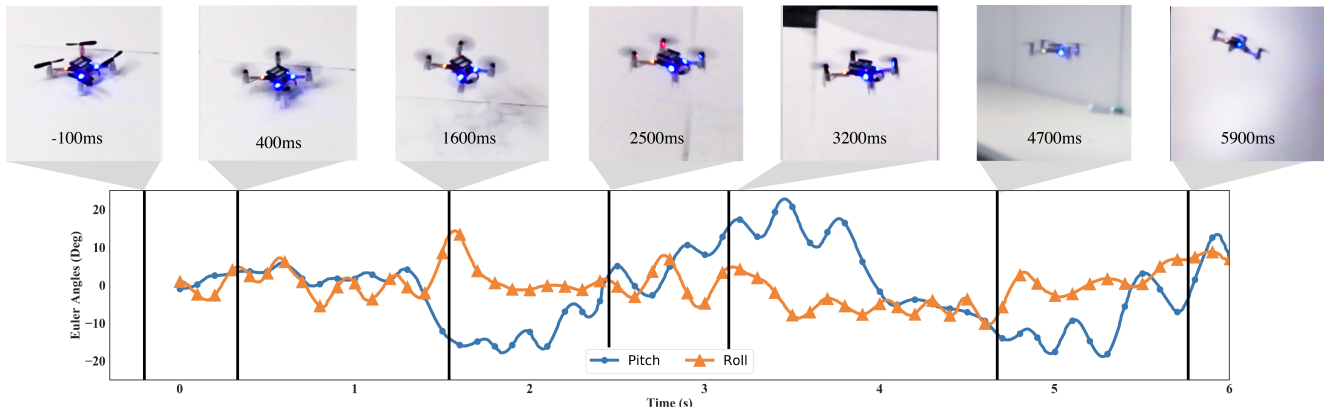


Fig. 9: A full flight of Euler angle state data with frames of the corresponding video. The relation between physical orientation and pitch and roll is visible in the frames. The full video is online on the accompanying website.

The broader benefits of this approach lay in its simplicity. The basis of comparison, typical quadrotor controllers, achieve better performance with higher control frequencies on-top of engineering design iterations by layering system dynamics knowledge. The initial results with MBRL should be compared to attitude only controllers until methods for drift correction are available on-board, such as the Crazyflie Flow Deck. In less than 10 minutes of clock time, and only 3 minutes of training data, we present comparable, but limited, performance that is encouraging for future abilities to match and surpass basic controllers. Moving the balance of this work further towards domain specific control would likely improve performance, but the broad potential for applications to more robots compels exciting future use of model-based reinforcement learning.

VII. CONCLUSIONS AND FUTURE WORK

This work is an exploration of the capabilities of model-based reinforcement learning for low-level control of an unknown system. The results, with the added challenges of the passive instability and fast dynamics of the Crazyflie, express the current capabilities of MBRL and highlight potential for future use. We demonstrate the firmware modifications, system design, and model learning considerations required to enable the use of a MBRL-based MPC system for the control of a quadrotor over radio. We removed all robot-specific transforms and higher level commands (e.g. thrust and Euler angle rate setpoints) to only design the controller on top of a learned dynamics model to accomplish a simple task. The controller shows the capability to hover for multiple seconds at a time off of less than 3 minutes of collected data – approximately half of the full battery life flight time of a Crazyflie quadrotor. The successful hovering of a quadrotor underscores potential extensions of the presented MBRL framework for future low-level control. With learned flight in only minutes of testing, this brand of system-agnostic MBRL is an exciting solution not due to its generalizability, but also due to its speed.

There are multiple pathways to investigate for improving the performance of the current system. Currently, the random

shooter MPC method devotes a substantial amount of computation on action samples that will never produce a desirable state change. Improving the precision of this sampling would improve sampling effectiveness and potentially performance. In the computationally limited case, an alternate approach should be taken to remove the online dynamics models predictions such as training a policy as an imitative model predictive controller or as a offline RL policy.

The results create opportunities for future implementations of the MBRL methodology and research into improvements for the algorithm. First, as demonstrated in this paper and in [3], MBRL can be used to control robots at a low-level and impels applications to other robots. With the use-cases learning entirely from experience in their infancy, each additional employment will likely uncover control or learning considerations needed for different classes of robots that can inform more fields than exclusively MBRL. The emergent area of microrobotics combines the issues of under-characterized actuators and dynamics, weak or non-existent controllers, “fast” system dynamics and therefore instabilities, and extremely high cost-to-test [29]–[31], so it is a strong candidate for MBRL experiments. Additionally, considerations to improve computational efficiency and predictive power warrant exploring future work on the method in simulation or basic experiment. Defining safety constraints within the model predictive controller, rather than just a safety kill-switch in firmware, could enable safe model learning, opening the door for fully autonomous learned control start to finish. Especially with safety addressed, with multiple similar robots, training can be run in parallel and the related dynamics models can be used as a weighted ensemble for prediction, hopefully decreasing total training time and improving performance. In conveying the ready potential for improvement, we hope to see additional engagement of model-based reinforcement learning research to accelerate the applications of any RL to robotics.

ACKNOWLEDGMENT

The authors thank the UC Berkeley Sensor & Actuator Center (BSAC), Berkeley DeepDrive, and Nvidia Inc.

REFERENCES

- [1] M. P. Deisenroth, D. Fox, and C. E. Rasmussen, "Gaussian processes for data-efficient learning in robotics and control," *IEEE Transactions on Pattern Analysis and Machine Intelligence*, vol. 37, no. 2, pp. 408–423, Feb 2015.
- [2] K. Chua, R. Calandra, R. McAllister, and S. Levine, "Deep Reinforcement Learning in a Handful of Trials using Probabilistic Dynamics Models," *Neural Information Processing Systems*, 2018.
- [3] A. Nagabandi, G. Yang, T. Asmar, G. Kahn, S. Levine, and R. S. Fearing, "Neural network dynamics models for control of under-actuated legged millirobots," *Intelligent Robots and Systems (IROS)*, 2018.
- [4] J. Hwangbo, I. Sa, R. Siegwart, and M. Hutter, "Control of a Quadrotor with Reinforcement Learning," *IEEE Robotics and Automation Letters*, vol. 2, no. 4, pp. 2096–2103, 2017.
- [5] S. Bansal, A. K. Akametalu, F. J. Jiang, F. Laine, and C. J. Tomlin, "Learning quadrotor dynamics using neural network for flight control," *2016 IEEE Conference on Decision and Control (CDC)*, pp. 4653–4660, 2016.
- [6] M. Deisenroth, D. Fox, and C. Rasmussen, "Gaussian processes for data-efficient learning in robotics and control," *IEEE Transactions on Pattern Analysis and Machine Intelligence (PAMI)*, vol. 37, no. 2, pp. 408–423, 2015.
- [7] G. Williams, N. Wagener, B. Goldfain, P. Drews, J. M. Rehg, B. Boots, and E. A. Theodorou, "Information theoretic MPC for model-based reinforcement learning," in *International Conference on Robotics and Automation (ICRA)*, 2017.
- [8] R. Mahony, V. Kumar, and P. Corke, "Multirotor aerial vehicles," *IEEE Robotics and Automation Magazine*, vol. 20, no. 32, 2012.
- [9] D. Mellinger, N. Michael, and V. Kumar, "Trajectory generation and control for precise aggressive maneuvers with quadrotors," *The International Journal of Robotics Research*, vol. 31, no. 5, pp. 664–674, 2012.
- [10] W. Zhang, M. W. Mueller, and R. D'Andrea, "A controllable flying vehicle with a single moving part," *2016 IEEE International Conference on Robotics and Automation (ICRA)*, pp. 3275–3281, 2016.
- [11] M. W. Mueller and R. D'Andrea, "Stability and control of a quadcopter despite the complete loss of one, two, or three propellers," *2014 IEEE International Conference on Robotics and Automation (ICRA)*, pp. 45–52, 2014.
- [12] M. Ryll, H. H. Bühlhoff, and P. R. Giordano, "Modeling and control of a quadrotor uav with tilting propellers," *2012 IEEE International Conference on Robotics and Automation (ICRA)*, pp. 4606–4613, 2012.
- [13] H. Liu, D. Li, J. Xi, and Y. Zhong, "Robust attitude controller design for miniature quadrotors," *International Journal of Robust and Nonlinear Control*, vol. 26, no. 4, pp. 681–696, 2016.
- [14] M. Bangura, R. Mahony, et al., "Real-time model predictive control for quadrotors," 2014.
- [15] M. Abdolhosseini, Y. Zhang, and C. A. Rabbath, "An efficient model predictive control scheme for an unmanned quadrotor helicopter," *Journal of intelligent & robotic systems*, vol. 70, no. 1-4, pp. 27–38, 2013.
- [16] A. P. Schoellig, F. L. Mueller, and R. DAndrea, "Optimization-based iterative learning for precise quadcopter trajectory tracking," *Autonomous Robots*, vol. 33, no. 1-2, pp. 103–127, 2012.
- [17] C. Sferrazza, M. Muehlebach, and R. D'Andrea, "Trajectory tracking and iterative learning on an unmanned aerial vehicle using parametrized model predictive control," *2017 IEEE Conference on Decision and Control (CDC)*, pp. 5186–5192, 2017.
- [18] P. Bouffard, A. Aswani, and C. Tomlin, "Learning-based model predictive control on a quadrotor: Onboard implementation and experimental results," *2012 IEEE International Conference on Robotics and Automation (ICRA)*, pp. 279–284, 2012.
- [19] T. Koller, F. Berkenkamp, M. Turchetta, and A. Krause, "Learning-based model predictive control for safe exploration and reinforcement learning," *arXiv preprint arXiv:1803.08287*, 2018.
- [20] F. Berkenkamp, A. P. Schoellig, and A. Krause, "Safe controller optimization for quadrotors with gaussian processes," *2016 IEEE International Conference on Robotics and Automation (ICRA)*, pp. 491–496, 2016.
- [21] S. Bansal, R. Calandra, T. Xiao, S. Levine, and C. J. Tomlin, "Goal-driven dynamics learning via bayesian optimization," *2017 IEEE Conference on Decision and Control (CDC)*, pp. 5168–5173, 2017.
- [22] I. Clavera, A. Nagabandi, R. S. Fearing, P. Abbeel, S. Levine, and C. Finn, "Learning to adapt: Meta-learning for model-based control," *arXiv preprint arXiv:1803.11347*, 2018.
- [23] A. Kupcsik, M. P. Deisenroth, J. Peters, A. P. Loh, P. Vadakkepat, and G. Neumann, "Model-based contextual policy search for data-efficient generalization of robot skills," *Artificial Intelligence*, vol. 247, pp. 415–439, 2017.
- [24] P. Abbeel, *Apprenticeship learning and reinforcement learning with application to robotic control*. Stanford University, 2008.
- [25] A. Punjani and P. Abbeel, "Deep learning helicopter dynamics models," in *IEEE International Conference on Robotics and Automation (ICRA)*, May 2015, pp. 3223–3230.
- [26] A. Bitcraze, "Crazyflie 2.0," 2016.
- [27] D. P. Kingma and J. Ba, "Adam: A method for stochastic optimization," *arXiv preprint arXiv:1412.6980*, 2014.
- [28] P. Ramachandran, B. Zoph, and Q. V. Le, "Swish: a self-gated activation function," *arXiv preprint arXiv:1710.05941*, 2017.
- [29] D. S. Drew, N. O. Lambert, C. B. Schindler, and K. S. Pister, "Toward controlled flight of the ionocraft: A flying microrobot using electrohydrodynamic thrust with onboard sensing and no moving parts," *IEEE Robotics and Automation Letters*, vol. 3, no. 4, pp. 2807–2813, 2018.
- [30] D. S. Contreras, D. S. Drew, and K. S. Pister, "First steps of a millimeter-scale walking silicon robot," *2017 International Conference on Solid-State Sensors, Actuators and Microsystems (TRANSDUCERS)*, pp. 910–913, 2017.
- [31] R. J. Wood, B. Finio, M. Karpelson, K. Ma, N. O. Pérez-Arancibia, P. S. Sreetharan, H. Tanaka, and J. P. Whitney, "Progress on picoair vehicles," *The International Journal of Robotics Research*, vol. 31, no. 11, pp. 1292–1302, 2012.

VIII. APPENDIX

A. Battery Voltage Context

The Crazyflie has a short battery voltage of about 7 minutes of flight time and operation depends heavily on battery voltage, with it becoming uncontrollable on low voltages when operating on our controllers or the built in nested PID controllers. In this experiment, we study the influence of the battery voltage to the dynamics of the Crazyflie, to understand if there is a time-varying drift that need to be compensated. We investigate this hypothesis by logging battery voltage and adding it to the state passed to the neural network during model training to improve prediction accuracy.

When operating the Crazyflie at control frequencies of greater than 100 Hz, the state dynamics become clearly biased at battery voltages less than 3,650 mV. The biases are present at lower frequencies, but less pronounced. The biased state dynamics can be seen in Figure 10, but the predictions do not improve when passing the battery voltage into the neural network dynamics model at any battery level. The RMS error delta between a model trained with and without battery voltage is less than 1%, indicating that the battery voltage is nearly completely captured in other variables

passed to the network.

A potential explanation for the lack of model improvement with logged battery voltage is that the current battery reading is latent in other variables past into the network, and the natural charge based variations in data are not dominant. The logged data shows a clear inverse relationship between battery voltage and current Crazyflie thrust, shown in Figure 12. The impedance of the motors changes depending on the rotor speed and drive. This battery and thrust relationship is less likely to be apparent on quadrotors with separate motor voltage controllers, where the impedance of the motors changing with revolutions per minute would be compensated for.

B. Crazyflie Lifespan

Extended periods of testing on individuals quadrotors demonstrated a finite lifetime. After many flights, performance would dip inexplicably. This is due to a combination of motor damage and or sensor decay. Motor damage causes a measureable change in the equilibrium PWMs for a given quadrotor. Figure 11 shows the change in the noise on the gyroscope before takeoff for all of the flights taken by the quadcopter used to collect data for this publication. The left

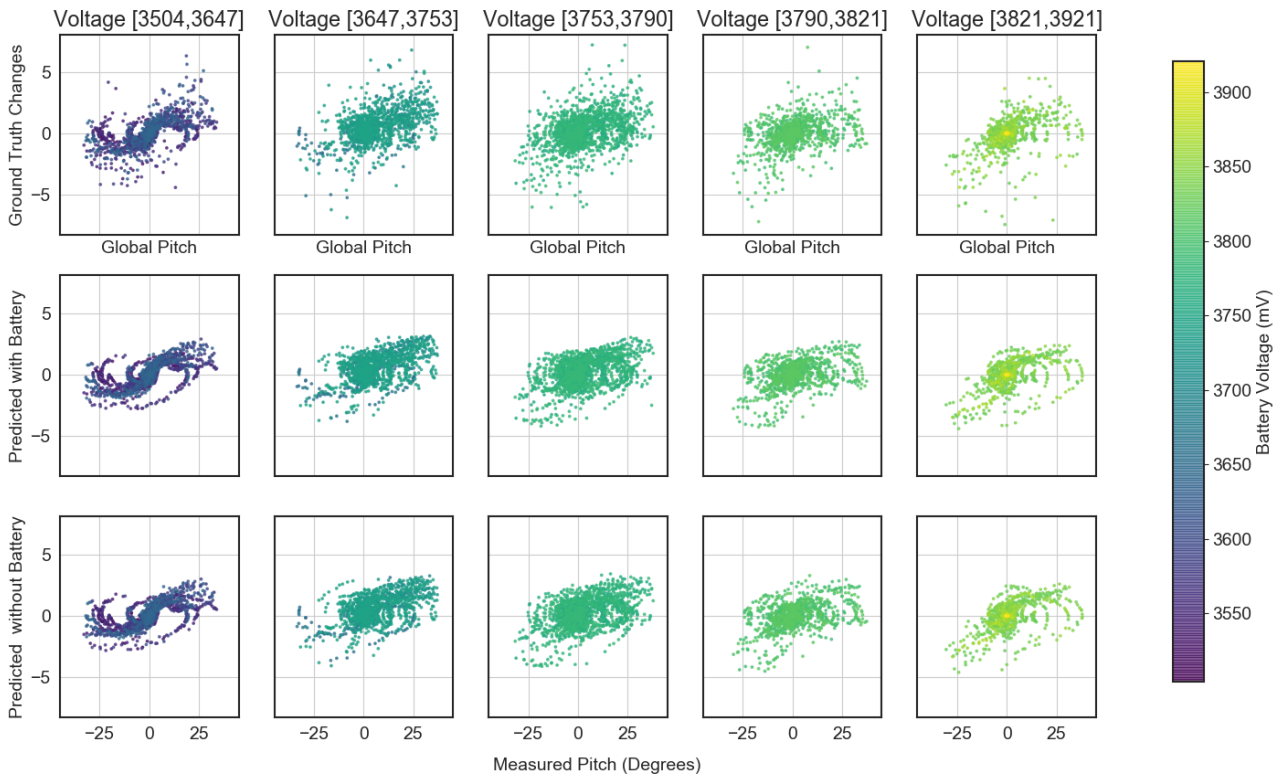


Fig. 10: Demonstration of the effect of battery voltage on state predictions. The top row is the ground truth one step pitch changes, the middle is the predictions through a model trained with battery voltage included in the state, and the bottom is predictions without battery voltage included in the state. Both of the predictions show tighter grouping from the variance term on the probabilistic loss function, but there is an extremely low difference between the predictions with and the predictions without battery. The lack of difference in predictions indicates the battery voltage is latent to other variables passed into the network.

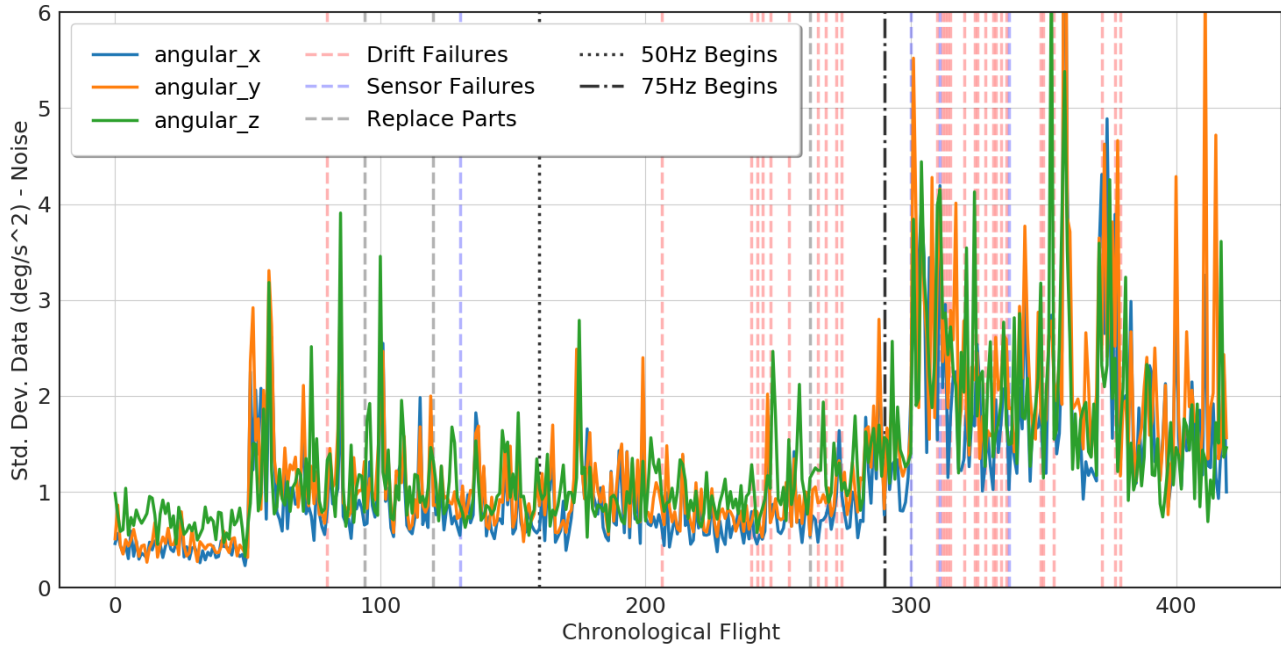


Fig. 11: The sensor noise on the 3 angular accelerations measured by the gyroscope of the MPU9250 of the Crazyflie before the robot takes off. The black vertical lines separate the rollouts at 25 Hz, 50 Hz and 75 Hz from left to right. The vertical lines indicate changes in hardware and collisions that would change the dynamics or state of the robot. The sensors clearly are subject to increasing noise over lifespan.

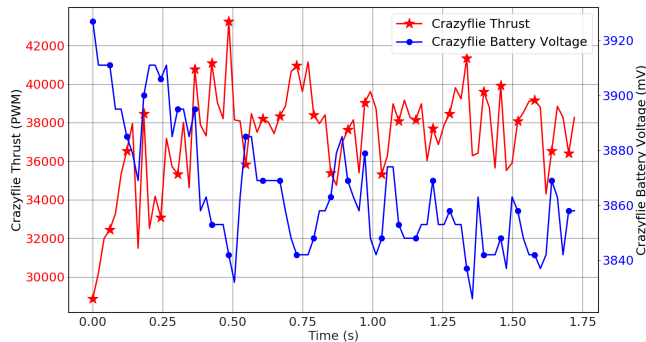


Fig. 12: The logged battery voltage and mean PWM of the 4 motors across a flight. There is a clear inverse relationship between the logged battery voltage and the current thrust.

two sections includes the data included in VI, but the data taken at a control frequency of 75 Hz was abandoned due to inconsistent performance. Some initial flights at 75 Hz were extremely promising, but after a series of collisions via drift the quadrotor would not take off cleanly. Future work should investigate methods of mitigating the effect of sensor drift, potentially by conditioning the dynamics model on a sensor noise measurement or enforcing more safety constraints on flight.

C. Frequency Dependent Learning

There is a trend between learned performance at both frequencies and the number of trained points for the model,

as shown in Figure 13. The continuing upward trend between logarithmic points and flight time indicates further data collection could enhance flight performance, but is unrealistic without further progress on safe learning with the Crazyflie. Potential future applications could leverage a combination of our results with bootstrapping data to continue to improve performance without the difficulties of logging large amounts of experimental data on an individual robot.

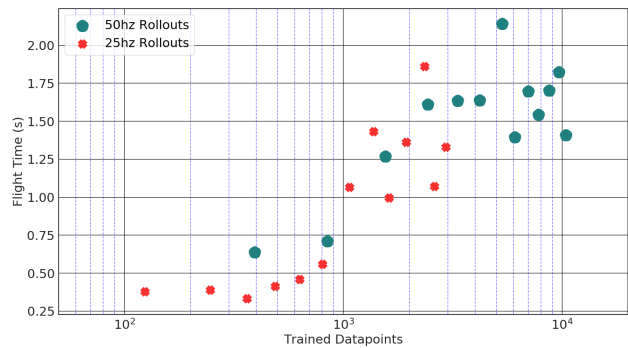


Fig. 13: Mean flight time of each rollout plotted versus the logarithm of the number of available points at train time for each model. The higher control frequency allows the controller to learn faster on wall time, but the plot indicates that there is not a notable difference between control ability when the number of trained points are equal. There is a continuing upward trend of flight time versus training points, but it is difficult to obtain more data in experiment.